J Neurol (2010) 257:721–727
DOI 10.1007/s00415-009-5396-8

ORIGINAL COMMUNICATION

Amyloid PET in mild cognitive impairment and Alzheimer's disease with BF-227: comparison to FDG–PET

Katsutoshi Furukawa · Nobuyuki Okamura · Manabu Tashiro · Masaaki Waragai · Shozo Furumoto · Ren Iwata · Kazuhiko Yanai · Yukitsuka Kudo · Hiroyuki Arai

Received: 6 June 2009 / Revised: 29 August 2009 / Accepted: 10 November 2009 / Published online: 28 November 2009

Abstract We recently developed a novel PET tracer, ^{11}C-labeled 2-(2-[2-dimethylaminothiazol-5-yl]ethenyl)-6-(2-[fluoro]ethoxy)benzoxazole ([^{11}C]BF-227), and had success with in vivo detection of amyloid plaques in Alzheimer's disease (AD) brains (Kudo et al. in J Nucl Med 8:553–561, 2007). We applied this tracer to subjects with mild cognitive impairment (MCI) and AD in order to elucidate the status of amyloid plaque deposition in MCI and compared the diagnostic performance of BF-227-PET with that of FDG–PET in AD cases. We studied 12 aged normal (AN) subjects, 15 MCIs and 15 ADs with PET using [^{11}C]BF-227. PET images were obtained after administration of BF-227 and the regional standardized uptake value (SUV) and the ratio of regional to cerebellar SUV were calculated as an index of BF-227 binding. AD patients showed increased uptake of [^{11}C]BF-227 in the neocortical areas and striatum as well as decreased glucose metabolism in temporoparietal, posterior cingulate and medial temporal areas. MCI subjects showed a significant increase in BF-227 uptake in the neocortical areas similar to AD, and the most significant difference of BF-227 retention was observed in the parietal lobe if its retentions for MCI were compared to those for AD and AN. On the other hand, glucose hypometabolism in MCI was confined to cingulate and medial temporal cortices. Neocortical BF-227 uptake negatively correlated with glucose metabolism. Receiver operating characteristic (ROC) analysis indicated higher specificity and sensitivity with BF-227-PET than those with FDG–PET for differential diagnosis between AD and normal control. We conclude that [^{11}C]BF-227-PET has a possibility to be a useful technology for early detection of AD pathology and also even in the MCI stage.

Keywords Alzheimer's disease · Amyloid · Senile plaque · PET · MCI

K. Furukawa and N. Okamura equally contributed to the article.

K. Furukawa (✉) · M. Waragai · H. Arai
Department of Geriatrics and Gerontology,
Division of Brain Sciences, Institute of Development,
Aging and Cancer, Tohoku University,
4-1 Seiryomachi, Aobaku, Sendai 980-8498, Japan
e-mail: kfurukawa-ns@umin.ac.jp

N. Okamura · S. Furumoto · K. Yanai
Department of Pharmacology,
Tohoku University Graduate School of Medicine,
4-1 Seiryomachi, Aobaku, Sendai 980-8575, Japan

M. Tashiro
Division of Cyclotron Nuclear Medicine,
Cyclotron and Radioisotope Center, 6-3Aoba,
Aramaki, Aoba-ku, Sendai, Miyagi 980-8578, Japan

R. Iwata
Division of Radiopharmaceutical Chemistry,
Cyclotron and Radioisotope Center, 6-3Aoba,
Aramaki, Aoba-ku, Sendai, Miyagi 980-8578, Japan

Y. Kudo
Department of NeuroImaging Research,
Innovation New Biomedical Engineering Center,
Tohoku University, 4-1 Seiryomachi, Aobaku,
Sendai 980-8498, Japan

Introduction

Senile or amyloid plaque is a pathological hallmark of Alzheimer's disease (AD), and amyloid β peptide (Aβ), which is a main component of the senile plaque, is believed to play a key role in the pathogenesis of AD [8]. In recent years several laboratories, including ours, have succeeded in visualizing Aβ deposition in living patients' brains with

AD using PET probes [13, 14, 24]. Pittsburgh Compound-B (PIB), which is the most commonly used probe for Aβ now, has been applied not only to AD but also to several other neurological disorders [15, 24].

Petersen from the Mayo clinic addressed the concept of mild cognitive impairment (MCI), which is an intermediate state between normal aging and AD [20, 21]. The criteria he stated for MCI are cognitive concern expressed by a physician, informant, participant or nurse; cognitive impairment in one or multiple domains (executive function, memory, language or visuospatial); normal functional activities; not demented.

Regional cerebral glucose metabolism (rCMRglu) has been studied by several investigators [9, 18, 19] using [^{18}F] 2-fluoro-deoxy-D-glucose (FDG) and PET in diseases causing dementia including AD. We used BF-227-PET as well as FDG–PET on the same subjects (AN, MCI, and AD) and carefully analyzed and compared the results with these two kinds of PET. Finally using these data we investigated and compared the specificity and sensitivity of BF-227 PET and FDG–PET in diagnosing AD.

Method

Twelve ANs, 15 subjects with MCI and 15 patients with AD were recruited in the present study. The demographic information of the subjects is shown in Table 1. The diagnosis for MCI and probable AD followed the MCI clinical criteria presented by "Petersen et al." [20] and "the National Institute of Neurological and Communicative Disorders and Stroke—Alzheimer's Disease and Related Disorders Association" [17], respectively. In 15 MCI subjects, 10 were amnestic multi-domain MCI and the other 5 subjects were amnestic single-domain MCI. Mini-mental state examination (MMSE) scores were significantly different between "AN and MCI", "AN and AD", and "MCI and AD". The study protocol was approved by the Committee on Clinical Investigation at Tohoku University School of Medicine and the Advisory Committee on Radioactive Substances at Tohoku University. After a complete description of the study to the patients and subjects, written informed consent was obtained.

Table 1 Demographic details of the subjects in this study

	N	Gender	Age	MMSE
AN	12	M/F = 7/5	66.3 ± 3.3	29.9 ± 0.3
MCI	15	M/F = 8/7	78.3 ± 3.8	25.5 ± 2.5
AD	15	M/F = 5/10	72.5 ± 6.9	19.5 ± 3.7

AN aged normal, *MCI* mild cognitive impairment, *AD* Alzheimer's disease. MMSE scores are significantly different between "AN and MCI", "AN and AD", and "MCI and AD"

The PET procedure for BF-227 was described precisely before [14]. BF-227 and its *N*-desmethylated derivative (a precursor of [^{11}C]BF-227) were custom-synthesized by Tanabe R&D Service Co. [^{11}C]BF-227 was synthesized from the precursor by *N*-methylation in dimethyl sulfoxide using [^{11}C]methyl triflate. The [^{11}C]BF-227 PET study was performed using a PET SET-2400 W scanner (Shimadzu Inc., Japan). After intravenous injection of 211–366 mBq of [^{11}C]BF-227, dynamic PET images were obtained for 60 min with each subject's eyes closed. Standardized uptake value (SUV) images of [^{11}C]BF-227 were obtained by normalizing tissue radioactivity concentration by injected dose and body weight. The FDG–PET procedure was described previously [19]. Subjects were scanned in a quiet and dimly-lit room with their eyes closed after at least 4 h of food restriction. Following a 68 Ga/Ga transmission scan of 7 min duration, an emission scan, which lasted 60 min after intravenous injection of FDG, was performed. The emission data were corrected for tissue attenuation using the transmission data. Regions of interest (ROIs) were placed on individual axial magnetic resonance (MR) images in the cerebellar hemisphere, striatum, frontal, lateral temporal, medial temporal, parietal, occipital, anterior and posterior cingulate cortices. The ROI information was then copied onto dynamic PET SUV images, and regional SUVs were sampled using Dr. View/LINUX software (AJS inc., Japan). Because there were neither senile plaques nor glucose hypometabolism in the cerebellum of AD, ratios of regional SUV to cerebellar SUV (SUVR) were calculated as an index of [^{11}C]BF-227 retention and CMRglu. Neocortical SUVR was calculated by averaging SUVRs in the frontal, lateral temporal, parietal and posterior cingulate cortices.

For statistical comparison in the three groups, we applied one-way analysis of variance (ANOVA) followed by the Bonferroni-Dunn post hoc test. The performance of diagnostic indices to discriminate among groups was assessed using the ROC analysis. Areas under ROC curves (AUC) were calculated and compared using GraphPad Prism Software (GraphPad Software Inc., San Diego, CA). Statistical significance was defined as $p < 0.05$.

Results

BF-227 retention in MCI

First, we analyzed PET images with [^{11}C]BF-227 among the three groups (AN, MCI, and AD), and representative brain PET images are shown in Fig. 1. As indicated in the figure, some MCI subjects showed strong retention of [^{11}C]BF-227, but other MCI subjects did not. Most AD cases, however, indicated strong accumulation of [^{11}C]BF-227 especially in

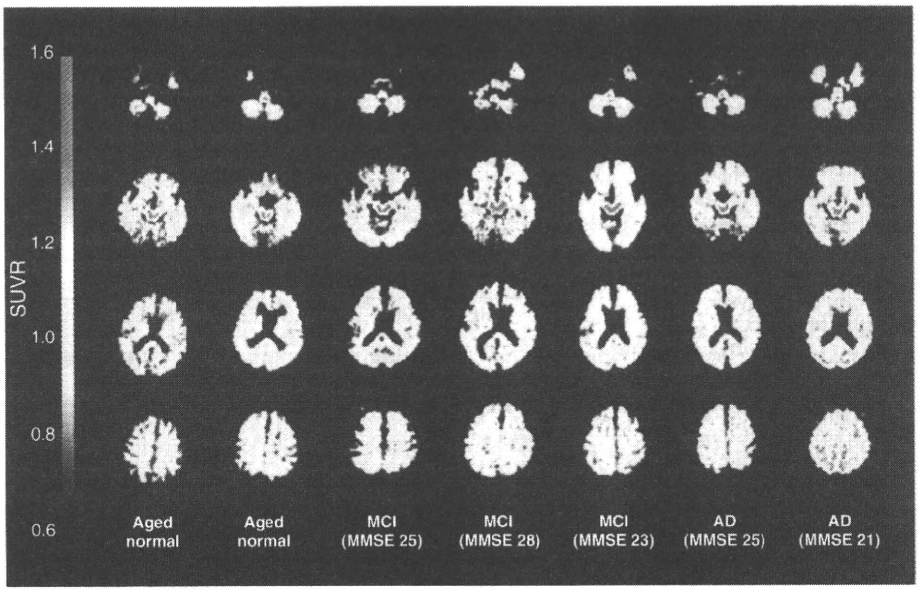

Fig. 1 Representative axial brain PET images with BF-227. Both the AD cases showed high SUVR compared to the aged normal subjects, although the MCI cases showed heterogeneity, that is, one MCI case (MMSE = 25) showed a comparative SUVR level to AN but another case showed SUVR as high as the AD level

frontal, temporal and parietal cortices. If the retention pattern of [^{11}C]BF-227 is compared to that of PIB, the accumulation of [^{11}C]BF-227 in the frontal lobe looks much weaker than that of PIB [3].

Figure 2 shows the mean neocortical and regional SUVRs of [^{11}C]BF-227 for the three groups. Both the mean neocortical SUVRs for MCI and AD are significantly higher than that for AN. As we previously reported [1], significantly higher SUVRs were observed in most cerebral regions in AD compared to AN except for the medial temporal lobe. MCI subjects indicated a significantly increased SUVR in frontal, lateral temporal, parietal, occipital cortices as well as anterior cingulate gyrus compared to AN, and the most prominent increase was observed in the lateral temporal cortex. A significantly lower SUVR in MCI was observed in the parietal cortex compared to AD. In the other neocortical regions, MCI subjects showed a tendency towards milder retention of BF-227 than that in AD. In the relationship between BF retentions and MMSE scores in all the subjects together (NC, MCI, and AD), no strong correlations were observed (data not shown).

Cerebral glucose metabolism in AN, MCI and AD

Next, we analyzed CMRglu in the same subjects using FDG–PET in order to compare to the findings with [^{11}C]BF-227, which is considered to indicate amyloid plaque depositions. As a result, a significant reduction of neocortical SUVR was observed in both MCI and AD patients compared to AN in FDG–PET (Table 1; Fig. 3). Regional SUVR in FDG–PET was significantly decreased in the cingulate gyrus and medial temporal cortex of MCI subjects and in the lateral temporal, parietal, posterior cingulate and medial temporal cortices of AD patients, compared to AN. Table 2.

Neocortical SUVR of FDG–PET for each subject was plotted against neocortical SUVR of BF-227-PET (Fig. 4a). SUVR of BF-227 negatively correlated to SUVR of FDG in analyzing the subjects from three groups all together ($r = -0.337$, $p = 0.029$). A significant correlation of regional SUVR in BF-227-PET and FDG–PET was also observed in the temporal and parietal cortices (data not shown). However, no significant correlation was observed when the analysis was confined to the subjects in each group.

Furthermore, in order to compare sensitivity and specificity to differentiate AD from AN, ROC analysis was performed for the lateral temporal SUVR of BF-227 and posterior cingulate SUVR of FDG (Fig. 4b). The AUC for BF-227 (0.994) is much higher than that for FDG (0.839), indicating that BF-227 is more sensitive as well as more specific than FDG in diagnosing AD.

Discussion

Our group recently developed a novel PET tracer, BF-227, and has reported that this compound is able to selectively detect dense amyloid deposits including senile plaques primarily in the posterior association area of AD patients. In the present study we applied this tracer to MCI cases and concluded that the mean value for the MCI cases with BF-227 was intermittent between AN and AD. Also we clarified that BF-227-PET is a useful technology to distinguish early AD patients from AN compared to FDG–PET.

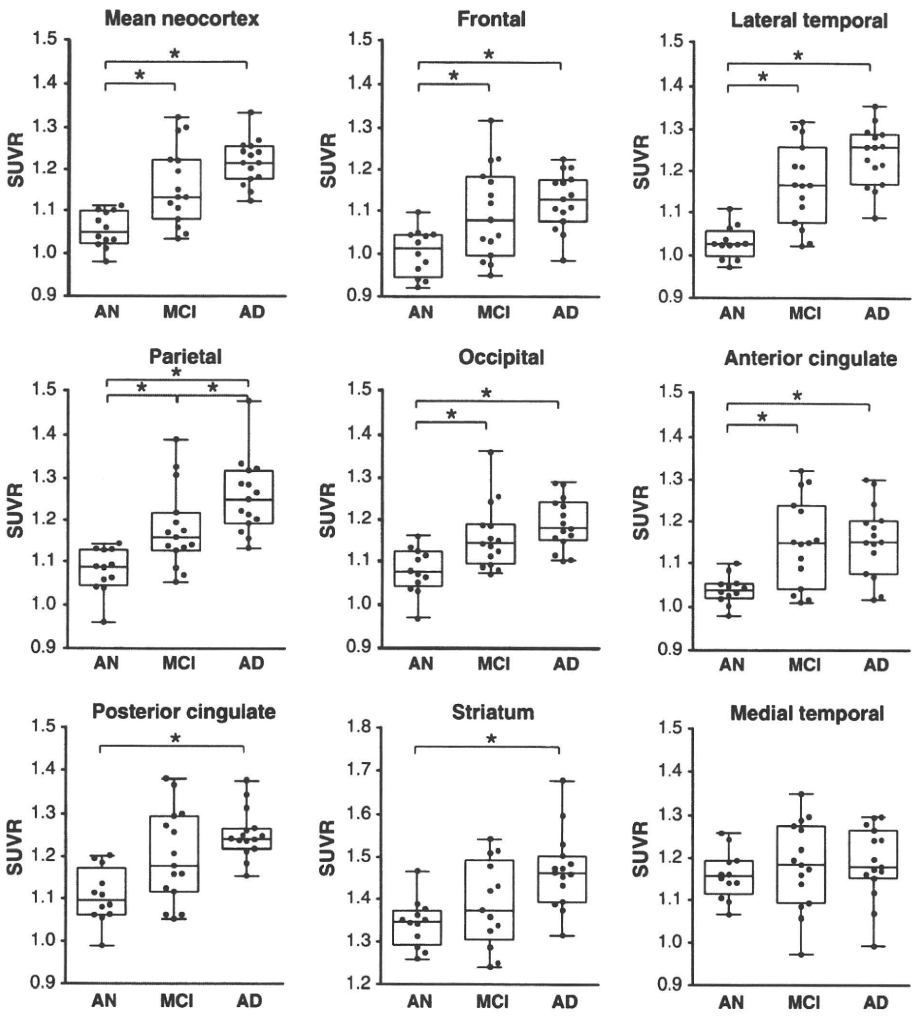

Fig. 2 Box plots of SUVR values with BF-227 PET for AN, MCI and AD. Each *dot* indicates the mean SUVR from "the mean neocortex" and "the eight regions", that is, frontal, temporal, parietal, occipital, anterior cingulate, posterior cingulated, striatum and medial temporal cortex. *Box* indicates interquartile range. *Vertical bars* indicate minimum–maximum range

MCI is now classified into 4 subtypes, that is, amnestic single-domain MCI, amnestic multi-domain MCI, non-amnestic single-domain MCI and non-amnestic multi-domain MCI. The important thing is that MCI (especially amnestic MCI) is regarded as a prodromal state of AD, in other words, a high percentage of MCI subjects are considered to convert to AD. It has been reported that 10–20% of MCI cases are going to convert to AD although only 1–2% of normal elderly convert to AD [21]. The present study concludes that MCI has high levels of [^{11}C]BF-227 retention indicating that senile plaque deposition already advances severely in the stage of MCI before dementia symptoms become obvious. Previous amyloid PET studies using ^{18}F-labeled 2-(1,1-dicyano-propen-2-yl)-6-(2-fluoroethyl)-methylamino-naphthalene (FDDNP) or PIB also indicated significant tracer retention in MCI and AD. Small et al. [24] presented that FDDNP can detect a high signal in MCI by binding not only for amyloid plaques but also tau neurofibrillary tangles, and the retention level for MCI is between AN and AD. On the other hand, several groups reported that about a half of the MCI subjects showed PIB uptake in the AD range, and other MCI subjects indicated retention levels lower than the AD range [12]. A group from Sweden concluded that MCI subjects who converted to AD later showed significantly higher PIB retention compared to non-converting MCI subjects and NC [6]. The present study also revealed higher retention of BF-227 in 60–70% of MCI subjects and in almost all the AD patients. Therefore, the amyloid PET technique is considered to be a highly useful and strong method for early detection of AD patients in the MCI stage. These pieces of information are indispensable in applying new treatment technologies against dementia into the prodromal stage of Alzheimer's disease. In other words, because it is considered that aggregation and deposition of Aβ starts much earlier before patients indicate symptoms of dementia, it is undoubtedly important to detect Aβ deposition as early as

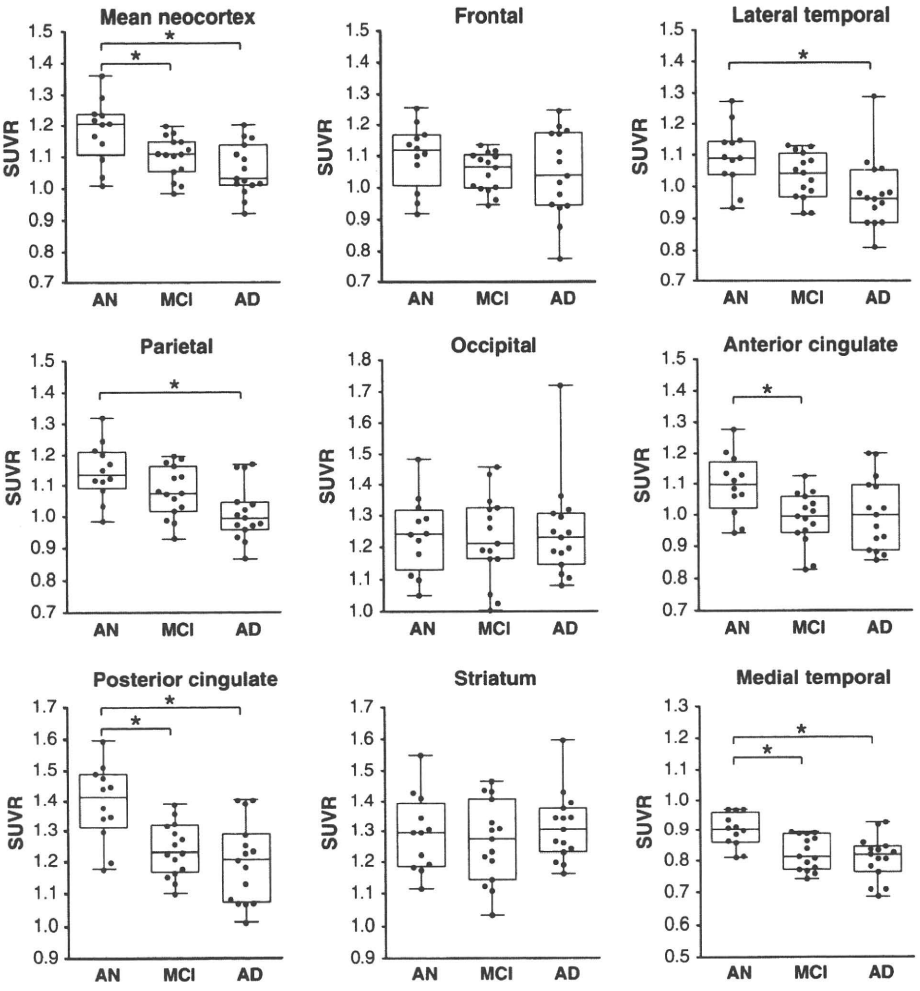

Fig. 3 Box plots of SUVR values with FDG–PET for AN, MCI and AD. Each *dot* indicates the mean SUVR from the mean neocortex and eight cerebral regions, that is, frontal, temporal, parietal, occipital, anterior cingulate, posterior cingulated, striatum and medial temporal cortex. *Boxes* indicate interquartile range. *Vertical bars* indicate minimum–maximum range

Table 2 Comparison of SUVR values of BF-227-PET and FDG–PET

		Mean neo cortex	Frontal	Lateral temporal	Parietal	Occipital	Anterior cingulate	Posterior cingulate	Striatum	Medial temporal
BF-227	AN	1.05 ± 0.04	1.00 ± 0.06	1.03 ± 0.04	1.08 ± 0.05	1.08 ± 0.05	1.04 ± 0.03	1.11 ± 0.07	1.34 ± 0.06	1.16 ± 0.06
	MCI	1.16 ± 0.10*	1.10 ± 0.11*	1.17 ± 0.10*	1.18 ± 0.10*	1.16 ± 0.08*	1.15 ± 0.11*	1.20 ± 0.11	1.41 ± 0.11	1.18 ± 0.10
	AD	1.22 ± 0.06*	1.13 ± 0.07*	1.24 ± 0.07*	1.25 ± 0.09*†	1.19 ± 0.06*	1.16 ± 0.09*	1.25 ± 0.06*	1.47 ± 0.09*	1.19 ± 0.09
FDG	AN	1.18 ± 0.10	1.10 ± 0.11	1.10 ± 0.10	1.15 ± 0.09	1.24 ± 0.12	1.10 ± 0.10	1.39 ± 0.13	1.29 ± 0.13	0.90 ± 0.06
	MCI	1.10 ± 0.06*	1.05 ± 0.06	1.03 ± 0.07	1.08 ± 0.08	1.23 ± 0.14	0.99 ± 0.08*	1.24 ± 0.09*	1.27 ± 0.13	0.82 ± 0.06*
	AD	1.06 ± 0.08*	1.05 ± 0.14	0.98 ± 0.11*	1.01 ± 0.09*	1.25 ± 0.15	1.00 ± 0.12	1.20 ± 0.13*	1.31 ± 0.11	0.81 ± 0.07*

Mean SUVR value for each brain region was obtained from AN, MCI and AD. * $p < 0.05$, versus AN, † $p < 0.05$ versus MCI

possible in order to begin medication to prevent or treat cognitive decline before the manifestations of dementia become clear.

In most PIB positive MCI and AD cases presented by several different laboratories, the frontal cortex showed high PIB retention, although the frontal cortex is not a region where amyloid plaques are predominantly rich in the early stage of AD or MCI according to the autopsy studies [1, 10]. Our newly developed tracer, BF-227, showed relatively high retention in temporal and parietal lobes for MCI and AD compared to the results with PIB. Since it is well known that the functional activity of the parietal lobe decreases in the early stage of AD [16], it is reasonable that the distribution of high BF-227-PET

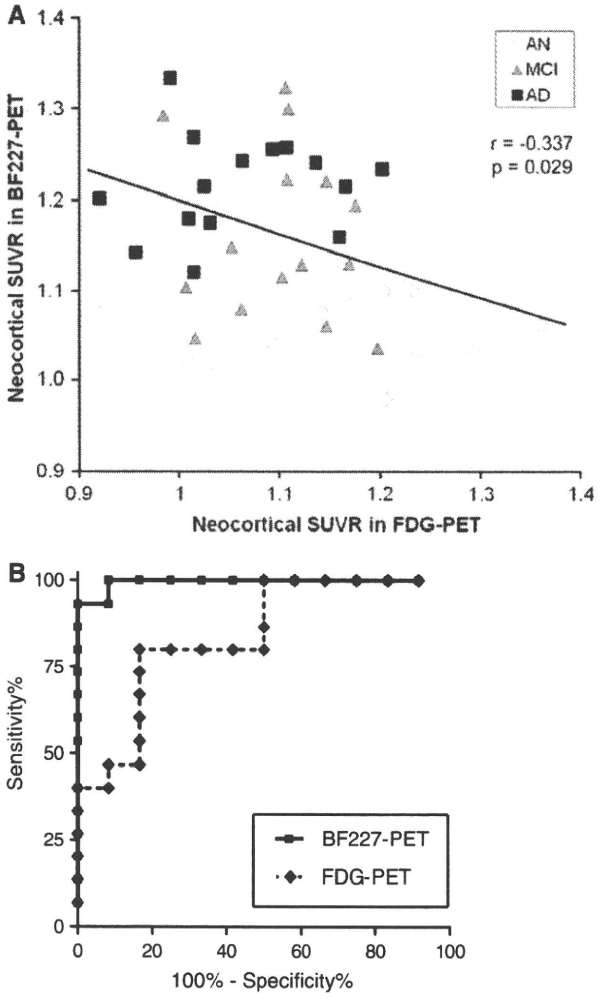

Fig. 4 **a** Relationship between neocortical SUVRs in FDG–PET and BF-227-PET. Neocortical SUVR of FDG–PET for each subject was plotted against neocortical SUVR of BF-227-PET. White, gray and black dots indicate AN, MCI and AD, respectively. **b** Receiver operating characteristic (ROC) curves of BF-227 and FDG–PET. BF-227-PET SUVR in the lateral temporal cortex and FDG–PET SUVR in the posterior cingulate cortex for differentiation between AD and AN

retention is closely related to the area indicating functional deterioration in the early stage of AD or MCI.

Low rCMRglu in AD especially in the posterior cingulate, precuneus, temporoparietal and frontal cortices was reported. FDG–PET has also been used in investigations for MCI, and low rCMRglu in the temporo-parietal and medial frontal cortices and hippocampus was reported as the most prominent predictor of subsequent cognitive decline [2–5]. Our results indicate, however, that amyloid retention detected by BF-227 is more sensitive and specific than FDG–PET for AD diagnosis. Therefore it is reasonable that amyloid PET is more sensitive than FDG–PET for detecting MCI, which is regarded as a prodromal state of dementia or early AD. According to previous autopsy studies with MCI, amyloid plaques were found predominantly in the temporal lobe structure and most amnestic MCI cases showed Braak stage II or III [11, 22]. Furthermore both neurofibrillary tangles and senile plaques were found in nondemented aging and "preclinical" AD, and profound neuronal loss was observed in layer II of the entorhinal cortex [7, 23]. Our results with BF-227 PET for MCI presented here agree with postmortem studies because BF-227 also showed high retention predominantly in the temporal lobe and the retention was intermittent between NC and AD. There are some discrepancies, however, between the results with our BF-227-PET and with autopsy, that is, some cerebral white matter, thalamus and pons showed high retention of BF-227 in MCI, although these regions are usually not rich in senile plaques in the autopsy studies. Although it is considered that the deposition of BF-227 in these regions comes from its non-specific retention by high lipophilicity, it is supposed that more precise studies are needed using more subjects for both PET and autopsy.

We now have to carefully consider the heterogeneity of BF-227 retention in MCI, which was also observed in FDDNP or PIB studies, that is, some subjects show rich retention but others do not. Although it was reported that MCI subjects showing high retention of PIB had a high tendency to convert to AD as we mentioned above [6], the number of subjects they examined was relatively small. Therefore, further careful studies are needed to clarify if the accumulation of amyloid PET probes correlates with the severity of cognitive impairment and a conversion rate to dementia.

Our results using BF-227 for MCI are "continuous" rather than "off/on", "negative/positive" or "dichotomous" signals compared to those with PIB. We speculate that because BF-227 can depict a small difference of amyloid deposition more finely than PIB, the results with BF-227 in MCI are more continuous than those with PIB. Therefore, BF-227 could reveal a degree of senile plaque deposition more precisely and accurately than PIB as far as in cases with MCI.

We would like to conclude that our newly developed amyloid PET tracer, BF-227, can detect amyloid aggregation and deposition in MCI cases and the PET signal intensity for MCI was intermittent between NC and AD. Results obtained with BF-227 PET are significantly more sensitive and specific than FDG–PET in diagnosing AD. As far as the retention pattern in the frontal and parietal cortices, BF-227 more accurately reflects senile plaque deposition observed in the autopsy studies than PIB does. Therefore, BF-227 PET should be an invaluable tool for diagnosis of AD in the early stage. Finally, we recently developed a novel probe, which has similar structure to BF-

227, labeled with F-18, and applied it to living humans. We have finished more than 20 cases so far and obtained similar results to BF-227.

Acknowledgments This study was supported by the Program for the Promotion of Fundamental Studies in Health Science by the National Institute of Biomedical Innovation, the Special Coordination Funds for Promoting Science and Technology, the Industrial Technology Research Grant Program from the New Energy and Industrial Technology Development Organization of Japan, Health and Labour Sciences Research Grants for Translational Research from the Ministry of Health, and the Ministry of Education, Culture, Sports and Technology. We appreciate technical assistance of Dr. Shoichi Watanuki and Dr. Yoichi Ishikawa in the clinical PET studies and Dr. Motohisa Kato in the imaging analysis.

References

1. Bennett DA, Cochran EJ, Saper CB, Leverenz JB, Gilley DW, Wilson RS (1993) Pathological changes in frontal cortex from biopsy to autopsy in Alzheimer's disease. Neurobiol Aging 14:589–596
2. Chételat G, Desgranges B, de la Sayette V, Viader F, Eustache F, Baron JC (2003) Mild cognitive impairment: Can FDG-PET predict who is to rapidly convert to Alzheimer's disease? Neurology 60:1374–1377
3. Chételat G, Eustache F, Viader F, De La Sayette V, Pélerin A, Mézenge F, Hannequin D, Dupuy B, Baron JC, Desgranges B (2005) FDG–PET measurement is more accurate than neuropsychological assessments to predict global cognitive deterioration in patients with mild cognitive impairment. Neurocase 11:14–25
4. de Leon MJ, Convit A, Wolf OT, Tarshish CY, DeSanti S, Rusinek H, Tsui W, Kandil E, Scherer AJ, Roche A, Imossi A, Thorn E, Bobinski M, Caraos C, Lesbre P, Schlyer D, Poirier J, Reisberg B (2001) Fowler et al. Prediction of cognitive decline in normal elderly subjects with 2-[(18)F]fluoro-2-deoxy-D-glucose/positron-emission tomography (FDG/PET). Proc Natl Acad Sci USA 98:10966–10971
5. Drzezga A, Lautenschlager N, Siebner H, Riemenschneider M, Willoch F, Minoshima S, Schwaiger M, Kurz A (2003) Cerebral metabolic changes accompanying conversion of mild cognitive impairment into Alzheimer's disease: a PET follow-up study. Eur J Nucl Med Mol Imaging 30:1104–1113
6. Forsberg A, Engler H, Almkvist O, Blomquist G, Hagman G, Wall A, Ringheim A, Långström B, Nordberg A (2008) A PET imaging of amyloid deposition in patients with mild cognitive impairment. Neurobiol Aging 29:1456–1465
7. Gómez-Isla T, Price JL, McKeel DW Jr, Morris JC, Growdon JH, Hyman BT (1996) Profound loss of layer II entorhinal cortex neurons occurs in very mild Alzheimer's disease. J Neurosci 16:4491–4500
8. Hardy J, Selkoe DJ (2002) The amyloid hypothesis of Alzheimer's disease: progress and problems on the road to therapeutics. Science 297:353–356
9. Herholz K, Carter SF, Jones M (2007) PET studies in dementia. Br J Radiol 80:S160–S167
10. Iwatsubo T, Odaka A, Suzuki N, Mizusawa H, Nukina N, Ihara Y (1994) Visualization of A beta 42(43) and A beta 40 in senile plaques with end-specific A beta monoclonals: evidence that an initially deposited species is A beta 42(43). Neuron 13:45–53
11. Jicha GA, Parisi JE, Dickson DW, Johnson K, Cha R, Ivnik RJ, Tangalos EG, Boeve BF, Knopman DS, Braak H, Petersen RC (2006) Neuropathologic outcome of mild cognitive impairment following progression to clinical dementia. Arch Neurol 63:674–681
12. Kemppainen NM, Aalto S, Wilson IA, Någren K, Helin S, Brück A, Oikonen V, Kailajärvi M, Scheinin M, Viitanen M, Parkkola R, Rinne JO (2007) PET amyloid ligand [11C]PIB uptake is increased in mild cognitive impairment. Neurology 68:1603–1606
13. Klunk WE, Engler H, Nordberg A, Wang Y, Blomqvist G, Holt DP, Bergström M, Savitcheva I, Huang GF, Estrada S, Ausén B, Debnath ML, Barletta J, Price JC, Sandell J, Lopresti BJ, Wall A, Koivisto P, Antoni G, Mathis CA, Långström B (2004) Imaging brain amyloid in Alzheimer's disease with Pittsburgh Compound-B. Ann Neurol 55:306–319
14. Kudo Y, Okamura N, Furumoto S, Tashiro M, Furukawa K, Maruyama M, Itoh M, Iwata R, Yanai K, Arai H (2007) 2-(2-[2-Dimethylaminothiazol-5-yl]ethenyl) -6-(2-[fluoro]ethoxy)benzoxazole: a novel PET agent for in vivo detection of dense amyloid plaques in Alzheimer's disease patients. J Nucl Med 8:553–561
15. Mathis CA, Klunk WE, Price JC, DeKosky ST (2005) Imaging technology for neurodegenerative diseases: progress toward detection of specific pathologies. Arch Neurol 62:196–200
16. Matsuda H (2007) Role of neuroimaging in Alzheimer's disease, with emphasis on brain perfusion SPECT. J Nucl Med 48:1289–1300
17. McKhann G, Drachman D, Folstein M, Katzman R, Price D, Stadlan EM (1984) Clinical diagnosis of Alzheimer's disease: report of the NINCDS-ADRDA Work Group under the auspices of Department of Health and Human Services Task Force on Alzheimer's Disease. Neurology 34:939–944
18. Minoshima S, Giordani B, Berent S, Frey KA, Foster NL, Kuhl DE (1997) Metabolic reduction in the posterior cingulate cortex in very early Alzheimer's disease. Ann Neurol 42:85–94
19. Okamura N, Arai H, Higuchi M, Tashiro M, Matsui T, Hu XS, Takeda A, Itoh M, Sasaki H (2001) [18F]FDG–PET study in dementia with Lewy bodies and Alzheimer's disease. Prog Neuropsychopharmacol Biol Psychiatry 25:447–456
20. Petersen RC, Smith GE, Waring SC, Ivnik RJ, Tangalos EG, Kokmen E (1999) Mild cognitive impairment: clinical characterization and outcome. Arch Neurol 56:303–308
21. Petersen RC (2004) Mild cognitive impairment as a diagnostic entity. J Intern Med 256:183–194
22. Petersen RC, Parisi JE, Dickson DW, Johnson K, Cha R, Ivnik RJ, Tangalos EG, Boeve BF, Knopman DS, Braak H, Petersen RC (2006) Neuropathologic features of amnestic mild cognitive impairment. Arch Neurol 63:665–672
23. Price JL, Morris JC (1999) Tangles and plaques in nondemented aging and "preclinical" Alzheimer's disease. Ann Neurol 45:358–368
24. Small GW, Kepe V, Ercoli LM, Siddarth P, Bookheimer SY, Miller KJ, Lavretsky H, Burggren AC, Cole GM, Vinters HV, Thompson PM, Huang SC, Satyamurthy N, Phelps ME, Barrio JR (2006) PET of brain amyloid and tau in mild cognitive impairment. N Engl J Med 355:2652–2663

doi:10.1093/brain/awq091 Brain 2010: 133; 1772–1778 | 1772

BRAIN
A JOURNAL OF NEUROLOGY

In vivo visualization of α-synuclein deposition by carbon-11-labelled 2-[2-(2-dimethylaminothiazol-5-yl)ethenyl]-6-[2-(fluoro)ethoxy]benzoxazole positron emission tomography in multiple system atrophy

Akio Kikuchi,[1] Atsushi Takeda,[1] Nobuyuki Okamura,[2] Manabu Tashiro,[3] Takafumi Hasegawa,[1] Shozo Furumoto,[2,4] Michiko Kobayashi,[1] Naoto Sugeno,[1] Toru Baba,[1] Yasuo Miki,[5] Fumiaki Mori,[5] Koichi Wakabayashi,[5] Yoshihito Funaki,[4] Ren Iwata,[4] Shoki Takahashi,[6] Hiroshi Fukuda,[7] Hiroyuki Arai,[8] Yukitsuka Kudo,[9] Kazuhiko Yanai[2] and Yasuto Itoyama[1]

1 Department of Neurology, Graduate School of Medicine, Tohoku University, Sendai, 980-8574 Japan
2 Department of Pharmacology, Graduate School of Medicine, Tohoku University, Sendai, 980-8575 Japan
3 Division of Cyclotron Nuclear Medicine, Cyclotron and Radioisotope Centre, Tohoku University, Sendai, 980-8578 Japan
4 Division of Radiopharmaceutical Chemistry, Cyclotron and Radioisotope Centre, Tohoku University, Sendai, 980-8578 Japan
5 Department of Neuropathology, Institute of Brain Science, Hirosaki University Graduate School of Medicine, Hirosaki, 036-8562 Japan
6 Department of Diagnostic Radiology, Graduate School of Medicine, Tohoku University, Sendai, 980-8575 Japan
7 Department of Nuclear Medicine and Radiology, Institute of Development, Ageing and Cancer, Tohoku University, Sendai, 980-8575 Japan
8 Department of Geriatric and Respiratory Medicine, Institute of Development, Ageing and Cancer, Tohoku University, Sendai, 980-8575 Japan
9 Innovation of New Biomedical Engineering Centre, Tohoku University, Sendai, 980-8574 Japan

Correspondence to: Atsushi Takeda,
Department of Neurology,
Graduate School of Medicine,
Tohoku University,
1-1 Seiryo-machi,
Aoba-ku, Sendai, Miyagi,
980-8574, Japan
E-mail: atakeda@em.neurol.med.tohoku.ac.jp

The histopathological hallmark of multiple system atrophy is the appearance of intracellular inclusion bodies, named glial cytoplasmic inclusions, which are mainly composed of α-synuclein fibrils. *In vivo* visualization of α-synuclein deposition should be used for the diagnosis and assessment of therapy and severity of pathological progression in multiple system atrophy. Because 2-[2-(2-dimethylaminothiazol-5-yl)ethenyl]-6-[2-(fluoro)ethoxy] benzoxazole could stain α-synuclein-containing glial cytoplasmic inclusions in post-mortem brains, we compared the carbon-11-labelled 2-[2-(2-dimethylaminothiazol-5-yl)ethenyl]-6-[2-(fluoro)ethoxy] benzoxazole positron emission tomography findings of eight multiple system atrophy cases to those of age-matched normal controls. The positron emission tomography data demonstrated high distribution volumes in the subcortical white matter (uncorrected $P<0.001$), putamen and posterior cingulate cortex (uncorrected $P<0.005$), globus pallidus, primary motor cortex and anterior cingulate cortex (uncorrected $P<0.01$), and substantia nigra (uncorrected $P<0.05$) in multiple system atrophy cases compared to the normal controls. They were coincident with glial cytoplasmic inclusion-rich brain areas in

Received January 13, 2010. Revised March 15, 2010. Accepted March 17, 2010. Advance Access publication April 29, 2010

multiple system atrophy and thus, carbon-11-labelled 2-[2-(2-dimethylaminothiazol-5-yl)ethenyl]-6-[2-(fluoro)ethoxy] benzoxazole positron emission tomography is a promising surrogate marker for monitoring intracellular α-synuclein deposition in living brains.

Keywords: glial cytoplasmic inclusion; Lewy body; β-amyloid; Parkinson's disease; Pittsburgh compound B

Abbreviations: BF-227 = 2-[2-(2-dimethylaminothiazol-5-yl)ethenyl]-6-[2-(fluoro)ethoxy]benzoxazole; MSA = multiple system atrophy; PIB = Pittsburgh compound B

Introduction

Multiple system atrophy (MSA) is a sporadic, progressive neurodegenerative disease characterized by variable severity of parkinsonism, cerebellar ataxia, autonomic failure and pyramidal signs. Although MSA was originally described as three separate diseases [olivopontocerebellar atrophy (Dejerine and Thomas, 1900), striatonigral degeneration (van der Eecken *et al.*, 1960) and Shy–Drager syndrome (Shy and Drager, 1960)], they are currently classified into a single disease that consists of MSA with predominant parkinsonism and MSA with predominant cerebellar ataxia (Gilman *et al.*, 1999). The histopathological hallmark of MSA, glial cytoplasmic inclusions, comprises mainly insoluble fibrils of phosphorylated α-synuclein (Wakabayashi *et al.*, 1998). Thus, it is suggested that the MSA is in the family of α-synucleinopathies (Marti *et al.*, 2003) including Parkinson's disease and dementia with Lewy bodies, which are characterized by the presence of Lewy bodies, representing other brain inclusions composed of α-synuclein.

Previous neuropathological studies indicated that the appearance of glial cytoplasmic inclusions preceded the clinical onset of MSA (Fujishiro *et al.*, 2008) and the amount of α-synuclein deposition correlated with the disease progression (Wakabayashi and Takahashi, 2006). Therefore, it is plausible that the formation of α-synuclein deposits plays a key role in neurodegeneration, and that compounds that inhibit this process may be therapeutically useful for MSA and other α-synucleinopathies. In fact some compounds, including antioxidants (Ono and Yamada, 2006) and non-steroidal anti-inflammatory drugs (Hirohata *et al.*, 2008), were reported to have potent anti-fibrillogenic and fibril-destabilizing effects on aggregated α-synucleins, and received much attention as possible new therapeutic agents (Ono and Yamada, 2006; Hirohata *et al.*, 2008). Detection of α-synuclein deposition *in vivo* could theoretically allow early diagnosis even at the presymptomatic stage, as well as assess disease progression and possible therapeutic effects in the living brain of patients with MSA.

Although Pittsburgh compound B (PIB) and other compounds were reported to be useful in detecting senile plaques *in vivo*, to our knowledge, there were no imaging probes currently available for *in vivo* detection of α-synuclein deposition. Recently, 2-[2-(2-dimethylaminothiazol-5-yl)ethenyl]-6-[2-(fluoro)ethoxy] benzoxazole (BF-227), known as a positron emission tomography (PET) probe for *in vivo* detection of dense β-amyloid deposits in humans (Kudo *et al.*, 2007), was reported to bind with synthetic α-synuclein aggregates as well as β-amyloid fibrils *in vitro* (Fodero-Tavoletti *et al.*, 2009). In the present study, we demonstrated that BF-227 could stain α-synuclein-containing glial cytoplasmic inclusions in post-mortem tissues and moreover, that a PET study with carbon-11-labelled BF-227 ([11C]-BF-227) could detect α-synuclein deposits in the living brains of patients with MSA.

Materials and methods

Neuropathological staining

Brain specimens

The subjects of the first part of the study were nine autopsy cases, including three with Parkinson's disease, three with dementia with Lewy bodies and three with MSA. The above diagnoses were confirmed both clinically and histopathologically. Brain tissues taken from the temporal cortex and substantia nigra of patients with Parkinson's disease and dementia with Lewy bodies, and pontine base of patients with MSA, were fixed in 20% buffered formalin for 72 h at 4°C, and vibratome sections (50 μm thick) were prepared.

Fluorescence and immunohistochemical analysis

BF-227 was dissolved in 50% ethanol containing 5% polysorbate (Tween 80; Wako, Osaka, Japan). The sections were slide mounted, incubated in 100 μM BF-227 for 30 min, dipped three times in phosphate buffer, and coverslipped with non-fluorescent mounting medium (Vectashield, Vector Laboratories, Burlingame, CA, USA). Fluorescence images were visualized using an Olympus Provis fluorescence microscope (Olympus, Tokyo, Japan) at wavelength 400 nm. After photographing fluorescent structures, BF-227-labelled sections were immunostained with primary antibodies against phosphorylated α-synuclein (#64; Wako). For phosphorylated α-synuclein immunohistochemistry, the sections were pre-treated with 99% formic acid for 5 min, then incubated overnight at 4°C with each primary antibody followed by incubation with the biotinylated secondary antibodies and the avidin–biotin–peroxidase complex (Vectastain ABC kit, Vector Laboratories). Diaminobenzidine was used as the chromogen.

PET study

Subjects

Eight patients with probable MSA and eight age-matched normal subjects were studied to examine the distribution of [11C]-BF-227 in the brain. All probable MSA patients were diagnosed on the second consensus criteria for probable MSA (Gilman *et al.*, 2008). Table 1 summarizes the clinical features of these patients. There were no significant differences in age, disease duration and unified MSA rating scale score between the MSA with predominant parkinsonism

Table 1 Subject profile

	Normal controls	MSA		
		Total	MSA-P	MSA-C
n	8	8	4	4
Gender (F/M)	4/4	4/4	1/3	3/1
Age (years)	64.3 ± 5.90	57.4 ± 10.1	60.5 ± 11.1	54.3 ± 9.50
Duration (years)		1.50 ± 0.54	1.75 ± 0.50	1.25 ± 0.50
UMSARS score		36.1 ± 8.87	41.5 ± 9.39	30.8 ± 4.27

Data are mean ± SD.
MSA-P = MSA with predominant parkinsonism; MSA-C = MSA with predominant cerebellar ataxia; UMSARS = unified MSA rating scale.

subgroup and the MSA with predominant cerebellar ataxia subgroup. The normal control group comprised volunteers without impairment of cognitive and motor functions who had no cerebrovascular lesions on magnetic resonance imaging. The study protocol was approved by the Ethical Committee of Tohoku University Graduate School of Medicine, and a written informed consent was obtained from each subject after being given a complete description of the study.

Radiosynthesis of [^{11}C]-BF-227

BF-227 and its N-desmethylated derivative (a precursor of [^{11}C]-BF-227) were custom-synthesized by Tanabe R&D Service Co. (Tokyo) (Kudo *et al.*, 2007). [^{11}C]-BF-227 was synthesized from the precursor by N-methylation in dimethyl sulphoxide using [^{11}C]-methyl triflate (Jewett, 1992; Iwata *et al.*, 2001). After quenching the reaction with 5% acetic acid in ethanol, [^{11}C]-BF-227 was separated from the crude mixture by semi-preparative reversed-phase high-performance liquid chromatography and then isolated from the collected fraction by solid-phase extraction. The purified [^{11}C]-BF-227 was solubilized in isotonic saline containing 1% polysobate-80 and 5% ascorbic acid. The saline solution was filter sterilized with a 0.22 mm Millipore® filter for clinical use. The radiochemical yields were >50% based on [^{11}C]-methyl triflate, and the specific radioactivities were 119–138 GBq/mmol at the end of synthesis. The radiochemical purities were >95%.

PET procedure

The [^{11}C]-BF-227 PET study was performed using a SET-2400W PET scanner (Shimadzu Inc., Japan) under resting condition with eyes closed in a dark room. Following a 68Ge/Ga transmission scan of 300–400 s duration, an emission scan was started soon after intravenous injection of 3.7–8.3 mCi of [^{11}C]-BF-227. A dynamic series of PET scans were acquired over 60 min with 23 frames. Emission data were corrected for attenuation, dead time and radioactive decay. Standardized uptake value images were obtained by normalizing tissue concentration by the injected dose and body mass. Arterial blood samples (1.5 ml) from the radial or brachial artery were collected from each subject at 10 s intervals for the first 2 min, and subsequently at intervals increasing progressively from 1 to 10 min until 60 min after the injection of [^{11}C]-BF-227 except for one subject, from whom arterialized venous blood samples (1.5 ml) from a hand vein heated in a far-infrared mat were collected at the same time intervals. The plasma obtained by centrifugation at 3000*g* for 3 min was weighed and the radioactivity was measured with a well-type scintillation counter. Additional arterial blood samples were obtained at four time points during the study (5, 15, 30 and 60 min) for the determination of radiolabelled metabolites in plasma using high-performance liquid chromatography. These data yielded values of the unchanged fraction of parent radiotracer throughout the time frame of the study. A multi-exponential equation was used to describe this curve and to estimate the parent fraction at each measured plasma curve time point.

PET image analysis

To measure α-synuclein deposition densities in the brain, the distribution volume, the ratio of [^{11}C]-BF-227 concentration in tissue to that in plasma at equilibrium, was calculated by Logan's graphical analysis (Logan, 2000), since BF-227 reversibly binds to α-synuclein depositions (Tashiro *et al.*, 2009). Region of interest analysis was performed to evaluate the regional distribution of [^{11}C]-BF-227. Circular regions of interest were placed on individual axial PET images in the frontal cortex, primary motor cortex, parietal cortex, medial temporal cortex, lateral temporal cortex, occipital cortex, anterior cingulate cortex, posterior cingulate cortex, subcortical white matter, caudate nucleus, putamen, globus pallidus, thalamus, substantia nigra, midbrain tegmentum, pons and cerebellar cortex, referring to the individual magnetic resonance images.

Statistical analysis

Data were expressed as mean ± SD. Differences in distribution volume between normal control and MSA groups were evaluated by one-way analysis of variance followed by Bonferroni's multiple comparison test (GraphPad Prism Software).

Results

Neuropathological staining

In the post-mortem brains with Parkinson's disease, double-labelling immunostaining with BF-227 fluorostaining and anti-phosphorylated α-synuclein antibody demonstrated co-localization of the proteins in Lewy bodies in the substantia nigra (Fig. 1A and B). Strong BF-227 staining was observed in the central core (Fig. 1A). BF-227 was also detected in the cortical Lewy bodies in dementia with Lewy bodies (Fig. 1C and D). In MSA, double-labelling experiments using BF-227 and anti-phosphorylated α-synuclein antibody demonstrated BF-227 fluorescent signal in the most of glial cytoplasmic inclusions in the pontine base (Fig. 1E and F).

PET study

Tissue time activity curves of [^{11}C]-BF-227 in the brain indicated more gradual clearance from the brain in patients with MSA compared with normal subjects following initial rapid uptake of radioactivity (Fig. 2A). Relatively high concentrations of [^{11}C]-BF-227 radioactivity were observed in the subcortical white matter and lenticular nucleus in MSA, in which relatively intense α-synuclein deposits were found in the post-mortem brain (Fig. 2B). [^{11}C]-BF-227 exhibited linear regression curves on Logan plot analysis in all brain regions examined. Since the slopes of the regression lines represent the distribution volume of the tracer, these findings indicated a higher distribution volume of [^{11}C]-BF-227 in MSA than in normal controls (Fig. 2C). The regional distribution volume values were high in the subcortical white matter (uncorrected $P<0.001$), putamen and posterior cingulate cortex

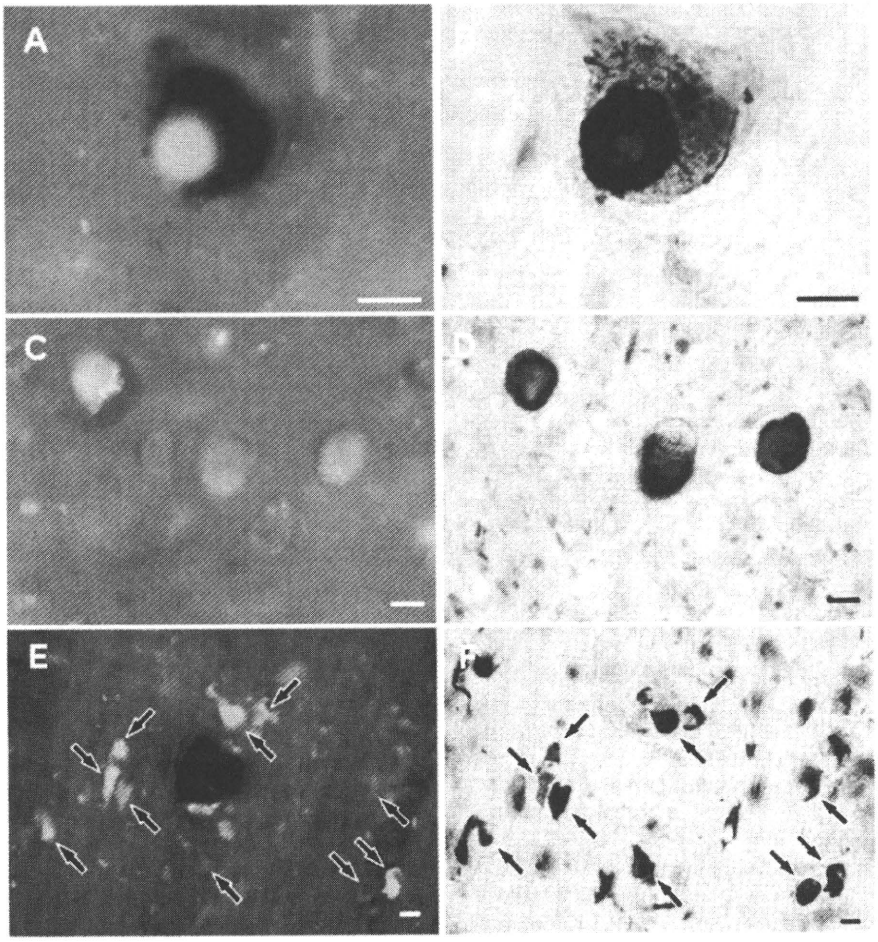

Figure 1 Neuropathological findings of BF-227 fluorostaining and anti-phosphorylated α-synuclein antibody immunostaining. BF-227 fluorostaining (**A** and **C**) and anti-phosphorylated α-synuclein antibody immunostaining (**B** and **D**) showed colocalization of these proteins in brainstem-type Lewy bodies in the substantia nigra of patients with Parkinson's disease (**A** and **B**) and in cortical Lewy bodies in the temporal lobe of patients dementia with Lewy bodies (**C** and **D**). Similarly, BF-227 fluorostaining (**E**) and anti-phosphorylated α-synuclein antibody immunostaining (**F**) were codetected in glial cytoplasmic inclusions in the pontine base of a patient with MSA. BF-227 histofluorescence was observed in the most of glial cytoplasmic inclusions (arrows). Bars = 10 μm.

(uncorrected $P<0.005$), globus pallidus, primary motor cortex and anterior cingulate cortex (uncorrected $P<0.01$) and substantia nigra (uncorrected $P<0.05$) in patients with MSA compared to the normal controls (Table 2 and Fig. 2D). It is noteworthy that the distribution volume of [^{11}C]-BF-227 was significantly high in the subcortical white matter even if Bonferroni's multiple comparison test was applied. On the other hand, no obvious differences were found in either the distribution or degree of binding between the MSA with predominant parkinsonism and MSA with predominant cerebellar ataxia subgroups.

Discussion

The BF-227 stained α-synuclein-containing Lewy bodies (Fig. 1A–D) and glial cytoplasmic inclusions (Fig. 1E and F) in formalin-fixed tissue sections as well as β-amyloid-containing senile plaques in paraffin-embedded tissue sections (Kudo *et al.*, 2007). These results were consistent with the previous findings showing BF-227 binding to synthetic α-synuclein fibrils with high affinity (K_d 9.63 nM) (Fodero-Tavoletti *et al.*, 2009), and to Lewy bodies in paraffin-embedded tissue sections (Fodero-Tavoletti *et al.*, 2009).

The anti-phosphorylated α-synuclein antibody immunostained the halo region more intensively compared with the central core in Lewy bodies in the substantia nigra of Parkinson's disease, while the BF-227 staining was intensely observed in the core of Lewy bodies (Fig. 1A and B). Because intense thioflavin S staining was also reported in the core of nigral Lewy bodies (Duda *et al.*, 2000), the core is thought to be rich in β-sheet structures. Similar to thioflavin S, the BF-227 staining is considered to recognize amyloid-like β-pleated sheets, and it was suggested to be the reason for the more intense BF-227 staining in the core of Lewy bodies. In addition, the high density of the core structure

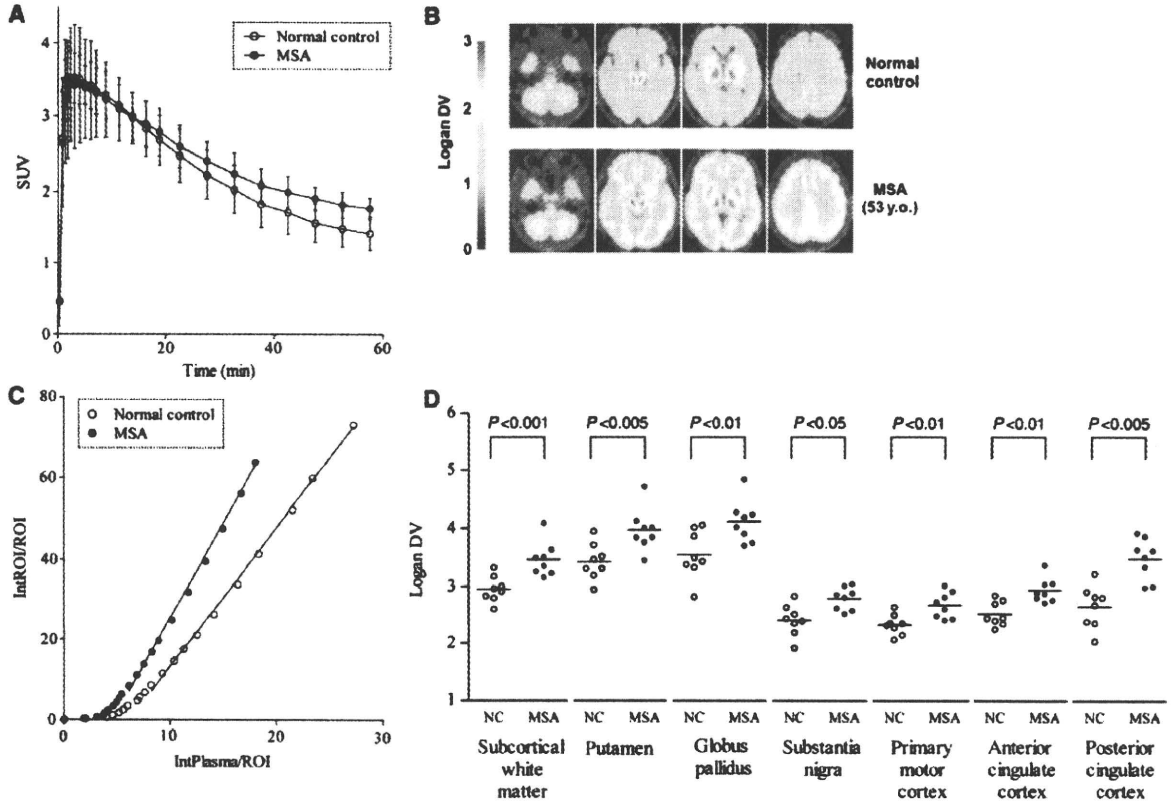

Figure 2 [^{11}C]-BF-227 PET findings in MSA. Time activity curves showed initial rapid uptake of radioactivity followed by gradual clearance in the putamen of both normal subjects and MSA cases. Data are mean ± SD of eight normal subjects and eight patients with MSA (**A**). In a representative patient with MSA with predominant cerebellar ataxia, the regional distribution volumes were mapped to the subcortical white matter and lentiform nucleus compared to normal control (**B**). Typical Logan plots for the putamen were presented in a representative patient with MSA with predominant cerebellar ataxia and a normal control. The slopes of the linear regression curves on Logan plot analysis represent the distribution volume of the tracer in the putamen (**C**). There were differences in the mean regional distribution volume values between patients with MSA and normal control in the subcortical white matter (uncorrected $P<0.001$), putamen and posterior cingulate cortex (uncorrected $P<0.005$), globus pallidus, primary motor cortex and anterior cingulate cortex (uncorrected $P<0.01$) and substantia nigra (uncorrected $P<0.05$). Data of individual subjects (symbols) and mean values (horizontal lines) (**D**). SUV = standardized uptake value; DV = distribution volume; ROI = region of interest.

may often prevent the penetration of antibodies into this region (Galloway *et al.*, 1992), since electron microscopic studies revealed that vesicular structures were tightly packed in the core of Lewy bodies (Takahashi and Wakabayashi, 2005). On the other hand, not all glial cytoplasmic inclusions stained by anti-phosphorylated α-synuclein antibody were always positive for BF-227 staining (Fig. 1E and F). In the process of oligodendroglial pathology, it was believed that α-synuclein deposits as amorphous state and then forms fibrillar structures (Gai *et al.*, 2003; Stefanova *et al.*, 2005). In fact, part of glial cytoplasmic inclusions were reported to be α-synuclein-negative (Sakamoto *et al.*, 2005) and therefore, it seems reasonable that some of glial cytoplasmic inclusions were not composed of β-sheet fibrils and were negative for BF-227 staining.

The regional distribution volume of [^{11}C]-BF-227 was the highest in the subcortical white matter, followed by the putamen, posterior cingulate cortex, anterior cingulate cortex, globus pallidus, primary motor cortex and substantia nigra, in which glial cytoplasmic inclusions were densely distributed (Papp and Lantos, 1994; Inoue *et al.*, 1997; Wakabayashi and Takahashi, 2006) and large increases of α-synuclein content were found (Tong *et al.*, 2010) in the post-mortem brains. Thus, it was suggested that the distributions of [^{11}C]-BF-227 could properly reflect those of the α-synuclein deposits *in vivo*. On the other hand, the regional distribution volume in other affected brain regions, such as the cerebellum and pons (Ozawa *et al.*, 2004; Wakabayashi and Takahashi, 2006), did not show higher values relative to the normal control group. The glial cytoplasmic inclusions in cerebellum were reported to decrease along with the disease progression and concomitant neuronal loss (Inoue *et al.*, 1997). Therefore, it is plausible that the accumulation levels of glial cytoplasmic inclusions are changing and do not always increase with the disease progression (Mochizuki *et al.*, 1992; Inoue *et al.*, 1997). Moreover, due to the remarkable cerebellar and pontine atrophy,

Table 2 Distribution volume of [11C]BF-227

	Normal controls	MSA
Frontal cortex	2.28 ± 0.18	2.46 ± 0.22
Primary motor cortex	2.40 ± 0.28	2.79 ± 0.20¶
Parietal cortex	2.48 ± 0.26	2.63 ± 0.24
Medial temporal cortex	2.44 ± 0.21	2.82 ± 0.31
Lateral temporal cortex	2.42 ± 0.19	2.63 ± 0.23
Occipital cortex	2.43 ± 0.20	2.72 ± 0.27
Anterior cingulate cortex	2.32 ± 0.18	2.67 ± 0.23¶
Posterior cingulate cortex	2.52 ± 0.22	2.94 ± 0.22†
Subcortical white matter	2.65 ± 0.38	3.49 ± 0.36‡
Caudate nucleus	2.70 ± 0.21	3.05 ± 0.34
Putamen	2.95 ± 0.23	3.47 ± 0.30†
Globus pallidus	3.43 ± 0.31	3.97 ± 0.36¶
Thalamus	3.50 ± 0.28	4.03 ± 0.31
Substantia nigra	3.55 ± 0.41	4.12 ± 0.36*
Midbrain tegmentum	3.53 ± 0.54	3.45 ± 0.47
Pons	3.63 ± 0.54	3.88 ± 0.42
Cerebellar cortex	2.32 ± 0.22	2.16 ± 0.29

Data are mean ± SD.
*Uncorrected $P < 0.05$.
¶Uncorrected $P < 0.01$.
†Uncorrected $P < 0.005$.
‡Uncorrected $P < 0.001$.

the distribution volume in these regions might be underestimated. Correction for partial volume loss is therefore needed to improve the accuracy of quantification in the cerebellum and brainstem of MSA. BF-227 fluorescent signal was detected in β-amyloid plaques as well as glial cytoplasmic inclusions and Lewy bodies (Fig. 1A–F) in neuropathological staining (Kudo *et al.*, 2007). However, the differences in the distribution of [11C]-BF-227 by PET could discriminate MSA from Alzheimer's disease, which showed high distribution of [11C]-BF-227 in the temporoparietal–occipital region (Kudo *et al.*, 2007). In our preliminary studies, Parkinson's disease and dementia with Lewy bodies also showed quite different patterns of distribution volumes from those of MSA (data not shown). Therefore, MSA could be distinguished from other degenerative diseases such as Alzheimer's disease, Parkinson's disease and dementia with Lewy bodies by the [11C]-BF-227 PET.

The affinity of BF-227 to α-synuclein fibrils (K_d 9.63 nM) was reported to be almost identical to that of PIB (K_d 10.07 nM) (Fodero-Tavoletti *et al.*, 2007, 2009). However, in the post-mortem human brain, the PIB binding was not colocalized with α-synuclein-positive Lewy bodies in two reports (Fodero-Tavoletti *et al.*, 2007; Ye *et al.*, 2008) although one report showed PIB binding to Lewy bodies in the substantia nigra of Parkinson's disease (Maetzler *et al.*, 2008). Therefore, there is controversy as to whether PIB binds to α-synuclein-containing Lewy bodies. Moreover, there have been no reports showing that PIB could detect α-synuclein deposits in α-synucleinopathies by PET (Fodero-Tavoletti *et al.*, 2007; Johansson *et al.*, 2008; Maetzler *et al.*, 2008). The hydroxy group in PIB (Mathis *et al.*, 2003) may prevent it from passing through the cell membranes and thereby detecting α-synuclein depositions in the cytoplasm, however, the BF-227 is more lipophilic than PIB (Mathis *et al.*, 2003), and may easily pass into the cytoplasm and bind to α-synuclein aggregates. As shown in the present study, BF-227 is a promising tracer to detect glial cytoplasmic inclusions. Further studies are warranted to verify whether Lewy bodies in other α-synucleinopathies as well as glial cytoplasmic inclusions can be detected by [11C]-BF-227 PET.

In conclusion, the BF-227 could bind to α-synuclein-containing glial cytoplasmic inclusions (Fig. 1E and F) in the post-mortem brain, and the [11C]-BF-227 PET demonstrated high signals in the glial cytoplasmic inclusion-rich brain regions including subcortical white matter, putamen, globus pallidus, primary motor cortex and anterior and posterior cingulate cortex (Table 2 and Fig. 2D). These results suggest that [11C]-BF-227 PET is a suitable surrogate maker for monitoring α-synuclein deposits in living brains with MSA and could be a potential tool to monitor the effectiveness of neuroprotective therapy for α-synucleinopathies.

Funding

Grant for 'the Research Committee for Ataxic Diseases' of the Research on Measures for Intractable Diseases from the Ministry of Health, Labour and Welfare, Japan (partial).

References

Dejerine J, Thomas A. L'atrophie olivo-ponto-cérébelleuse. Nouvelle Iconographie Salpêtrière 1900; 13: 330–7.

Duda JE, Lee VM, Trojanowski JQ. Neuropathology of synuclein aggregates. J Neurosci Res 2000; 61: 121–7.

Fodero-Tavoletti MT, Mulligan RS, Okamura N, Furumoto S, Rowe CC, Kudo Y, et al. In vitro characterisation of BF227 binding to alpha-synuclein/Lewy bodies. Eur J Pharmacol 2009; 617: 54–8.

Fodero-Tavoletti MT, Smith DP, McLean CA, Adlard PA, Barnham KJ, Foster LE, et al. In vitro characterization of Pittsburgh compound-B binding to Lewy bodies. J Neurosci 2007; 27: 10365–71.

Fujishiro H, Ahn TB, Frigerio R, DelleDonne A, Josephs KA, Parisi JE, et al. Glial cytoplasmic inclusions in neurologically normal elderly: prodromal multiple system atrophy? Acta Neuropathol 2008; 116: 269–75.

Gai WP, Pountney DL, Power JH, Li QX, Culvenor JG, McLean CA, et al. alpha-Synuclein fibrils constitute the central core of oligodendroglial inclusion filaments in multiple system atrophy. Exp Neurol 2003; 181: 68–78.

Galloway PG, Mulvihill P, Perry G. Filaments of Lewy bodies contain insoluble cytoskeletal elements. Am J Pathol 1992; 140: 809–22.

Gilman S, Low PA, Quinn N, Albanese A, Ben-Shlomo Y, Fowler CJ, et al. Consensus statement on the diagnosis of multiple system atrophy. J Neurol Sci 1999; 163: 94–8.

Gilman S, Wenning GK, Low PA, Brooks DJ, Mathias CJ, Trojanowski JQ, et al. Second consensus statement on the diagnosis of multiple system atrophy. Neurology 2008; 71: 670–6.

Hirohata M, Ono K, Morinaga A, Yamada M. Non-steroidal anti-inflammatory drugs have potent anti-fibrillogenic and fibril-destabilizing effects for alpha-synuclein fibrils in vitro. Neuropharmacology 2008; 54: 620–7.

Inoue M, Yagishita S, Ryo M, Hasegawa K, Amano N, Matsushita M. The distribution and dynamic density of oligodendroglial cytoplasmic inclusions (GCIs) in multiple system atrophy: a correlation between the density of GCIs and the degree of involvement of striatonigral and olivopontocerebellar systems. Acta Neuropathol 1997; 93: 585–91.

Iwata R, Pascali C, Bogni A, Miyake Y, Yanai K, Ido T. A simple loop method for the automated preparation of (11C)raclopride from (11C)methyl triflate. Appl Radiat Isot 2001; 55: 17–22.

Jewett DM. A simple synthesis of [11C]methyl triflate. Int J Rad Appl Instrum [A] 1992; 43: 1383–5.

Johansson A, Savitcheva I, Forsberg A, Engler H, Langstrom B, Nordberg A, et al. [(11)C]-PIB imaging in patients with Parkinson's disease: preliminary results. Parkinsonism Relat Disord 2008; 14: 345–7.

Kudo Y, Okamura N, Furumoto S, Tashiro M, Furukawa K, Maruyama M, et al. 2-(2-[2-Dimethylaminothiazol-5-yl]ethenyl)-6-(2-[fluoro]ethoxy)benzoxazole: a novel PET agent for in vivo detection of dense amyloid plaques in Alzheimer's disease patients. J Nucl Med 2007; 48: 553–61.

Logan J. Graphical analysis of PET data applied to reversible and irreversible tracers. Nucl Med Biol 2000; 27: 661–70.

Maetzler W, Reimold M, Liepelt I, Solbach C, Leyhe T, Schweitzer K, et al. [11C]PIB binding in Parkinson's disease dementia. Neuroimage 2008; 39: 1027–33.

Marti MJ, Tolosa E, Campdelacreu J. Clinical overview of the synucleinopathies. Mov Disord 2003; 18(Suppl): S21–7.

Mathis CA, Wang Y, Holt DP, Huang GF, Debnath ML, Klunk WE. Synthesis and evaluation of 11C-labeled 6-substituted 2-arylbenzothiazoles as amyloid imaging agents. J Med Chem 2003; 46: 2740–54.

Mochizuki A, Mizusawa H, Ohkoshi N, Yoshizawa K, Komatsuzaki Y, Inoue K, et al. Argentophilic intracytoplasmic inclusions in multiple system atrophy. J Neurol 1992; 239: 311–6.

Ono K, Yamada M. Antioxidant compounds have potent anti-fibrillogenic and fibril-destabilizing effects for alpha-synuclein fibrils in vitro. J Neurochem 2006; 97: 105–15.

Ozawa T, Paviour D, Quinn NP, Josephs KA, Sangha H, Kilford L, et al. The spectrum of pathological involvement of the striatonigral and olivopontocerebellar systems in multiple system atrophy: clinicopathological correlations. Brain 2004; 127: 2657–71.

Papp MI, Lantos PL. The distribution of oligodendroglial inclusions in multiple system atrophy and its relevance to clinical symptomatology. Brain 1994; 117(Pt 2): 235–43.

Sakamoto M, Uchihara T, Nakamura A, Mizutani T, Mizusawa H. Progressive accumulation of ubiquitin and disappearance of alpha-synuclein epitope in multiple system atrophy-associated glial cytoplasmic inclusions: triple fluorescence study combined with Gallyas-Braak method. Acta Neuropathol 2005; 110: 417–25.

Shy GM, Drager GA. A neurological syndrome associated with orthostatic hypotension: a clinical-pathologic study. Arch Neurol 1960; 2: 511–27.

Stefanova N, Reindl M, Neumann M, Haass C, Poewe W, Kahle PJ, et al. Oxidative stress in transgenic mice with oligodendroglial alpha-synuclein overexpression replicates the characteristic neuropathology of multiple system atrophy. Am J Pathol 2005; 166: 869–76.

Takahashi H, Wakabayashi K. Controversy: is Parkinson's disease a single disease entity? Yes. Parkinsonism Relat Disord 2005; 11(Suppl 1): S31–7.

Tashiro M, Okamura N, Furumoto S, Kumagai K, Furukawa K, Sugi K, et al. Quantitative analysis of amyloid deposition in Alzheimer's disease patients and healthy volunteers using PET and [11C]BF-227. In: Proceedings of the International Symposium on Early Detection and Rehabilitation Technology of Dementia 2009 (DRD2009). Okayama, Japan, 2009.110–1.

Tong J, Wong H, Guttman M, Ang LC, Forno LS, Shimadzu M, et al. Brain alpha-synuclein accumulation in multiple system atrophy, Parkinson's disease and progressive supranuclear palsy: a comparative investigation. Brain 2010; 133: 172–88.

van der Eecken H, Adams RD, van Bogaert L. Striopallidal-nigral degeneration. An hitherto undescribed lesion in paralysis agitans. J Neuropathol Exp Neurol 1960; 19: 159–61.

Wakabayashi K, Takahashi H. Cellular pathology in multiple system atrophy. Neuropathology 2006; 26: 338–45.

Wakabayashi K, Yoshimoto M, Tsuji S, Takahashi H. Alpha-synuclein immunoreactivity in glial cytoplasmic inclusions in multiple system atrophy. Neurosci Lett 1998; 249: 180–2.

Ye L, Velasco A, Fraser G, Beach TG, Sue L, Osredkar T, et al. In vitro high affinity alpha-synuclein binding sites for the amyloid imaging agent PIB are not matched by binding to Lewy bodies in postmortem human brain. J Neurochem 2008; 105: 1428–37.

Sleep Medicine 11 (2010) 100–101

Contents lists available at ScienceDirect

Sleep Medicine

journal homepage: www.elsevier.com/locate/sleep

Introduction to Images in Sleep Medicine

This section is intended to tap into a relatively unique feature of sleep science: images with great educational and conceptual content (e.g., electroencephalograms, electromyograms, polysomnograms, portable devices, actigrams, scans including functional images, pathology specimens, brain slice preparations, fluorescent microscopy and other cutting edge techniques). Please see our web site's (http://ees.elsevier.com/sleep/) **Guide for Authors** for instructions. We hope this section will be enriched by the contributions of our colleagues who wish to offer stimulating opportunities for discussion and new insights into the field of sleep.

doi:10.1016/S1389-9457(09)00442-0

Follow-up PET studies in case of idiopathic REM sleep behavior disorder

Tomoyuki Miyamoto [a,*], Satoshi Orimo [b], Masayuki Miyamoto [a], Koichi Hirata [a], Tomoko Adachi [b], Ryo Hattori [b], Masahiko Suzuki [c,d], Kenji Ishii [d]

[a] Department of Neurology, Center of Sleep Medicine, Dokkyo Medical University School of Medicine, Japan
[b] Department of Neurology, Kanto Central Hospital, Japan
[c] Department of Neurology, The Jikei University School of Medicine, Japan
[d] Positron Medical Center, Tokyo Metropolitan Institute of Gerontology, Japan

ARTICLE INFO

Article history:
Received 6 April 2009
Accepted 15 May 2009
Available online 9 July 2009

Keywords:
Idiopathic REM sleep behavior disorder
PET
Cardiac ^{123}I-MIBG scintigraphy
Parkinson's disease
Dementia with Lewy bodies
Neurodegenerative disease

1. Introduction

REM sleep behavior disorder (RBD) is a frequent feature of Parkinson's disease (PD) or dementia with Lewy bodies (DLB) and is characterized by dream-enacting behaviors, unpleasant dreams, and loss of muscle atonia during REM sleep [1]. Progression to PD or DLB has been reported in some patients with idiopathic RBD (iRBD) [1,2]. We followed the present case by PET immediately after development of iRBD and yearly for 2.5 years.

A 73-year-old man presented because of a history of distinct talking and falling out of bed during sleep beginning at around the age of 70 years. He had a history of sleep talk and feeling faint when standing up during the previous 6 years. Mild rigidity was noted in his right wrist and he had a slight frontal gait, but no bradykinesia or tremor. During the head-up tilt test blood pressure was 121/69 mmHg in the supine position and 99/49 mmHg in the upright position. In both the first (at 71 years) and second study (at 73 years), the heart-to-mediastinum (H/M) ratio was reduced (early 1.68, delayed 1.45; early 1.36, delayed 1.12, respectively) in ^{123}I-MIBG cardiac scintigraphy (MIBG) [3]. Polysomnography showed the REM sleep without atonia. RBD was defined according to criteria in the International Classification of Sleep Disorders, second edition.

2. Image analysis

The viability of presynaptic dopaminergic neurons was evaluated by PET with [^{11}C]carbomethoxy flurophenyl tropane (CFT). Activity was calculated using the ratio index [i.e., (target region of interest-cerebellum/cerebellum) and compared with results from healthy control subjects ($n = 6$, ages 57–74).

Activities of the right/left caudate, anterior putamen and posterior putamen of CFT were 3.63/3.70, 3.87/3.75 and 3.35/3.22, respectively, at age 71 one year after RBD onset and 3.27/3.13, 3.41/3.3 and 2.79/2.88, respectively, 2.5 years after the first scan. Rate of decrease (%) of right/left caudate, anterior putamen and posterior putamen per year was 3.95/6.45, 4.83/4.67 and 6.60/4.04, respectively (Fig. 1).

3. Discussion

Nigrostriatal presynaptic dopaminergic function was normal 1 year after diagnosis of iRBD and decreased by 4~6% per year,

* Corresponding author. Address: Dokkyo Medical University School of Medicine, 880 Kitakobayashi Mibu, Tochigi 321-0293, Japan.
E-mail address: miyatomo@dokkyomed.ac.jp (T. Miyamoto).

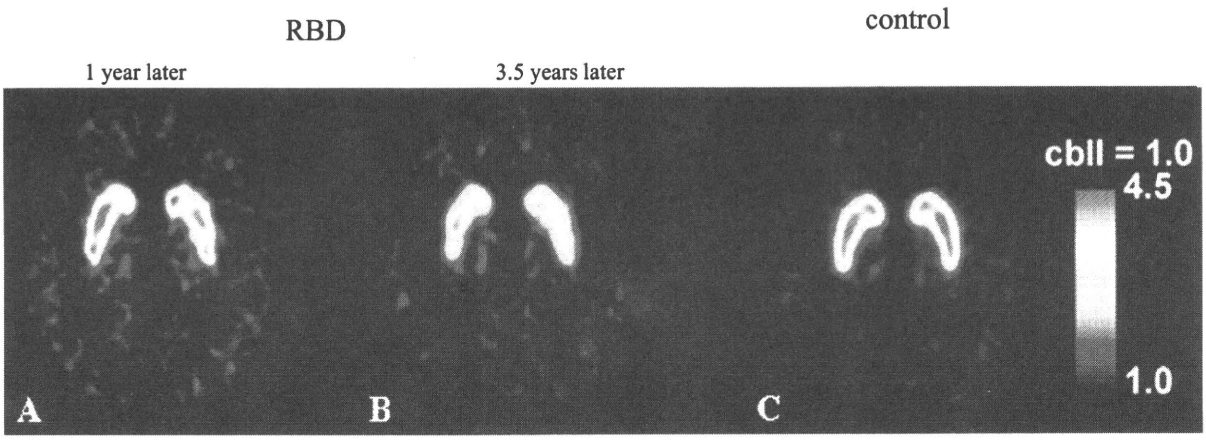

Fig. 1. Images of [^{11}C]carbomethoxy flurophenyl tropane: nigrostrial presynaptic dopaminergic function was almost normal except for a slight decrease in the left posterior putamen at 71 years (A: August 2004) compared with control subject (C), but decreased by 4–6% per year at 2.5 years after the first scan (B: January 2007).

which is similar to that in PD [4]. But reduced cardiac MIBG uptake and orthostatic hypotension had already appeared at the onset of iRBD, indicating that degeneration of non-motor neurons preceded that of motor neurons. We reported that cardiac MIBG uptake is reduced in patients with iRBD, suggesting that the cardiac sympathetic nerve involvement and lesions responsible for iRBD develop during the same period [3].

Few longitudinal published studies have addressed the natural course of iRBD. Eleven of 29 older men (38%) diagnosed with iRBD developed parkinsonian disorders within 3.7 years, and 17 of 26 patients (65.4%) developed the disease within 13 years of diagnosis of iRBD [1]. Twenty-six of 93 cases of iRBD progressed to neurodegenerative disease: 17.7% at 5 years; 40.6% at 10 years; and 52.4% at 12 years [2]. Onset of PD usually begins a few years to a little over a decade after the development of iRBD. Moreover, degeneration of the cardiac sympathetic nerve precedes involvement of nigrostriatal presynaptic dopaminergic function in RBD [5].

References

[1] Gagnon JF, Postuma RB, Mazza S, Doyon J, Montplaisir J. Rapid-eye movement sleep behavior disorder and neurodegenerative diseases. Lancet Neurol 2006;5:424–32.
[2] Postuma RB, Gagnon JF, Vendette M, Fantini ML, Massicotte-Marquez J, Montplaisir J. Quantifying the risk of neurodegenerative disease in idiopathic REM sleep behavior disorder. Neurology 2009;72:1296–300.
[3] Miyamoto T, Miyamoto M, Suzuki K, Nishibayashi M, Iwanami M, Hirata K. ^{123}I-MIBG cardiac scintigraphy provides clues to the underlying neurodegenerative disorder in idiopathic REM sleep behavior disorder. Sleep 2008;31:717–23.
[4] Nurmi E, Bergman J, Eskola O, Solin O, Vahlberg T, Sonninen P, et al. Progression of dopaminergic hypofunction in striatal subregions in Parkinson's disease using [18F]CFT PET. Synapse 2003;48:109–15.
[5] Eisensehr I, Linke R, Tatsch K, Kharraz B, Gildehaus JF, Wetter CT, et al. Increased muscle activity during rapid eye movement sleep correlates with decrease of striatal presynaptic dopamine transporters. IPT and IBZM SPECT imaging in subclinical and clinically manifest idiopathic REM sleep behavior disorder, Parkinson's disease, and controls. Sleep 2003;26:507–12.

doi: 10.1016/j.sleep.2009.05.006

Movement Disorders
Vol. 24, No. 12, 2009, pp. 1811–1819

Expanding the Clinical Phenotype of *SNCA* Duplication Carriers

Kenya Nishioka, MD, PhD,[1,2] Owen A. Ross, PhD,[2] Kenji Ishii, MD,[3] Jennifer M. Kachergus, BS,[2] Kiichi Ishiwata, PhD,[3] Mayumi Kitagawa, MD, PhD,[4] Satoshi Kono, MD, PhD,[5] Tomokazu Obi, MD, PhD,[6] Koichi Mizoguchi, MD, PhD,[6] Yuichi Inoue, MD, PhD,[7] Hisamasa Imai, MD, PhD,[8] Masashi Takanashi, MD, PhD,[1] Yoshikuni Mizuno, MD,[1] Matthew J. Farrer, PhD,[2] and Nobutaka Hattori, MD, PhD[1]*

[1]*Department of Neurology, Juntendo University School of Medicine, Bunkyo-ku, Tokyo, Japan*
[2]*Division of Neurogenetics, Department of Neuroscience, Mayo Clinic, Jacksonville, Florida, USA*
[3]*Tokyo Metropolitan Institute of Gerontology, Itabashi-ku, Tokyo, Japan*
[4]*Department of Neurology, Sapporo Azabu Neurosurgical Hospital, Higashi-ku, Sapporo, Japan*
[5]*Department of Neurology, Hamamatsu University School of Medicine, Shizuoka, Japan*
[6]*Department of Neurology, Shizuoka Institute of Epilepsy and Neurological Disorders, Shizuoka, Japan*
[7]*Japan Somnology Center, Neuropsychiatric Research Institute, Shibuya-ku, Tokyo, Japan*
[8]*Department of Neurology, Tokyo Rinkai Hospital, Edogawa-ku, Tokyo, Japan*

Abstract: *SNCA* duplication is a recognized cause of familial Parkinson's disease (PD). We aimed to explore the genetic and clinical variability in the disease manifestation. Molecular characterization was performed using real-time PCR, SNP arrays, and haplotype analysis. We further studied those patients who were found to harbor *SNCA* duplication with olfactory function tests, polysomnography, and PET. We identified four new families and one sporadic patient with *SNCA* duplication. Eleven symptomatic patients from these four families presented with parkinsonism, of which three subsequently developed dementia. The lifetime estimate of overall penetrance was 43.8%. FDG–PET study of symptomatic patients showed hypometabolism in the occipital lobe, whereas asymptomatic carriers of *SNCA* duplication demonstrated normal glucose metabolism. Symptomatic patients showed abnormal olfactory function and polysomnography and asymptomatic carriers showed normal results. The clinical features of *SNCA* duplication include parkinsonism with or without dementia. Asymptomatic carriers displayed normal test results with the eldest individual aged 79 years; thus, even a carrier of *SNCA* duplication may escape the development of PD. This difference in age-associated penetrance may be due to the genetic background or environmental exposures. Further studies of *SNCA* duplication carriers will help identify disease-modifiers and may open novel avenues for future treatment. © 2009 Movement Disorder Society

Key words: Parkinson's disease; *SNCA* duplication; PET; dementia; reduced penetrance

The cardinal features of Parkinson's disease (PD) include rest tremor, rigidity, bradykinesia, and postural instability. The pathologic hallmark is neuronal degeneration in the substantia nigra and locus coeruleus with Lewy bodies in the surviving neurons.[1] The reason for selective vulnerability and neuronal loss in sporadic PD is not known yet.

Mutations of the *SNCA* gene have been observed to result in familial PD with similar clinical and pathologic features to those present in the sporadic form of the disease. In addition to three coding substitutions in the α-synuclein protein (p.A30P, p.E46K, and p.A53T), genomic multiplication of chromosome 4q21-22, containing the *SNCA* locus has also been linked to autosomal dominant PD with or without dementia.[2–13] In contrast with the parkinsonism and dementia associated with *SNCA* triplication, clinical features of monoallelic duplication (three copies of *SNCA*) are

Additional Supporting Information may be found in the online version of this article.

*Correspondence to: Dr. Nobutaka Hattori, Department of Neurology, Juntendo University School of Medicine, 2-1-1 Hongo, Bunkyo-ku, Tokyo 113-8421, Japan. E-mail: nhattori@juntendo.ac.jp

Potential conflict of interest: The authors declare no financial or other conflicts of interest.

Received 28 January 2009; Revised 25 March 2009; Accepted 27 May 2009

Published online 26 June 2009 in Wiley InterScience (www.interscience.wiley.com). DOI: 10.1002/mds.22682

essentially those of sporadic PD without dementia, although generally with an earlier age at onset.[12,13] Recently, we reported a Japanese patient with parkinsonism and dementia resulting from *SNCA* duplication, who was pathologically diagnosed as diffuse Lewy body disease (DLBD).[14] These pathologic findings are reminiscent of those observed in some *SNCA* triplication patients.[15,16]

Herein, we report our screening of *SNCA* multiplication in both familial and sporadic PD patients, in which we found four new families and one apparently sporadic patient with *SNCA* duplication. Furthermore, within our families, we observed 14 asymptomatic carriers with *SNCA* duplication. We studied our patients and asymptomatic carriers with olfactory tests, brain MRI, PET using [^{11}C]-RAC, [^{11}C]-CFT, and [^{18}F]-FDG, and polysomnography (PSG). We report motor and nonmotor features as well as laboratory aspects of *SNCA* duplication in symptomatic and asymptomatic subjects.

SUBJECTS AND METHODS

Subjects of Gene Dosage Analysis

We studied 103 consecutive patients with autosomal dominant PD [43 male and 60 female with a mean age at onset of 50.9 ± 13.9 years (±SD)] who had at least one affected individual within one degree of separation, and 71 patients (29 male and 42 female with 37.7 ± 13.0 years) with sporadic PD. We reported Family A and B previously.[11] Diagnosis of PD was made according to the United Kingdom Parkinson's Disease Society Brain Bank criteria by participating neurologists (KN, YM, and NH).[17] All the patients studied were Japanese and a summary of the clinical data is presented in Table 1. The study was approved by the ethics review committee of Juntendo University. We obtained written informed consent from all the patients in whom blood samples were collected for genetic analyses.

Gene Dosage and Haplotype Analysis on *SNCA* Locus

DNA was prepared according to standard methods from peripheral blood.[18] Mutation screening was performed as previously described.[11] *SNCA* duplication was confirmed with copy number variation analysis using the Affymetrix 250K SNP array (Affymetrix, Santa Clara, CA) as described previously.[7] DNA samples for all available family members were genotyped for short tandem repeat markers flanking the *SNCA* locus (D4S3475, D4S3477, D4S3480, D4S3479, and D4S3474) using fluorescent-labeled primers, ABI PRISM 3730 DNA Analyzer, and Genemapper software version *4.0* (Applied Biosystems, CA). All PCR conditions, primer and probe sequences are available upon request.

PET Studies

Four symptomatic familial patients (A-II-9, A-II-11, C-III-3, and E-III-6), and three asymptomatic carriers (A-II-2, A-II-4, and A-III-3) were studied by [^{11}C]-labeled 2β-carbomethoxy-3β-(4-flurophenyl)-tropane (CFT) and [^{11}C]-labeled racroplide (RAC). Demographics of each group are shown in Table 2. We also examined comparison groups of sporadic PD patients with Hoehn and Yahr stage I (n = 10, male (m):female (f) = 5:5; mean age at exam 58.6 ± 9.57 years), stage II (n = 18, m:f = 9:9; CFT 66.6 ± 9.87 years; RAC 65.3 ± 9.22 years), and stage III disease (n = 9, m:f = 2:7; CFT 66.5 ± 10.3 years; RAC 65.8 ± 10.6 years), and normal controls (n = 7, m:f = 4:3; CFT; 59.4 ± 5.00 years; RAC; 60.9 ± 5.59 years). The same symptomatic familial patients and asymptomatic carriers, and an additional normal control group (n = 30, m:f = 12:18; 52.9 ± 3.9 years) were analyzed for [^{18}F]-labeled 2-fluoro-2-deoxy-D-glucose (FDG).

PET studies were performed in the Positron Medical Center, Tokyo Metropolitan Institute of Gerontology Positron Medical Center with a HEADTOME V scanner (Shimazu, Kyoto, Japan).[19] All anti-Parkinson drugs were discontinued for at least 12 hours before dopaminergic scanning. We used [^{11}C]-CFT for dopamine transporter imaging and [^{11}C]-RAC for dopamine receptor imaging; these imaging studies were performed on the same day. Cerebral glucose metabolism was evaluated with FDG on a different day within a week from the dopaminergic PET study.

PET image manipulations were carried out using the medical image processing application package "*Dr View/LINUX*" version *R2.0* (AJS, Tokyo, Japan) and SPM2 (The Wellcome Department of Imaging Neuroscience, Institute of Neurology, University College London, London, UK) implemented in *MATLAB* version *7.0.1* (MathWorks, Natick, MA). Regions of interest were placed on PET images with reference to individual co-registered MRI on the cerebral hemisphere, caudate nucleus, and striatum on each side. The activity was calculated using the ratio index (i.e., target region of interest activity—cerebellar activity/cerebellar activity) that is linearly correlated with the regional binding potential of [^{11}C]-CFT. For visual inspection, a

TABLE 1. *Clinical data of SNCA duplication patients*

Heredity	Autosomal dominant										Sporadic
SNCA duplication	A-II-9 (+)	A-II-11 (+)	B-II-7 (+)	C-III-3 (+)	D-III-1 (+)	D-III-5 (+)	E-III-4 (+)	E-III-6 (+)	F-II-5 (+)	F-III-2 (+)	G-III-1 (+)
Gender/age at last exam	F/58	M/44	M/67	F/57	F/57	M/46	F/66	M/57	M/68	M/40	M/35
Age at onset	48	38	47	49	56	38	54	53	62	37	31
Symptom at onset	Gait disturbance	Gait disturbance	Rigidity on the left hand	Bradykinesia on right hand	Bradykinesia on right hand	Bradykinesia on left hand	Bradykinesia	Bradykinesia on right hand	Rigidity on right hand	Tremor on left hand	Bradykinesia on right hand
DD	10	7	21	9	2	9	13	5	7	4	5
UPDRS (on)	28/199	37/199	Bed ridden	20/199	17/199	31/199	95/199	23/199	58/199	17/199	13/199
Hoehn and Yahr stage (on)	III	III	V	III	II	II	V	II	III	II	II
MMSE	28/30	26/30	0/30	27/30	30/30	30/30	7/30	28/30	19/30	30/30	28/30
HDSR	29/30	24/30	0/30	27/30	30/30	29/30	8/30	28/30	19/30	29/30	30/30
Beck	32	20	(−)	5	0	1	(−)	4	10	15	24
Hamilton	14	9	(−)	6	0	1	(−)	0	15	12	29
Hallucination or delusion	(+)	(−)	(++)	(−)	(−)	(−)	(+++)	(−)	(++)	(+)	(+)
Olfactory dysfunction	(+)	(+)	NK	(+)	NK	NK	NK	(+)	NK	(+)	(+)
RBD	(+)	(+)	NK	(−)	(−)	(−)	NK	(−)	NK	(−)	(+)
Response to levodopa	Moderate	Moderate	Early good, Later no effect	Moderate	Good	Good	Early good, Later no effect	Good	Poor	Good	Good

Clinical symptoms of 11 patients were assessed. Rigidity and akinesia are the main symptoms, and tremor was less problematic. Dementia and severe cognitive decline was observed in three patients (B-II-7, E-III-4, and F-II-5). Hallucination was also a marked symptom (6/11).

M, male; F, female; NK, not known; DD, disease duration; UPDRS, unified Parkinson's disease rating scale; H and Y stage, Hoehn and Yahr stage; MMSE, mini-mental state examination; HDS-R, revised Hasegawa dementia scale; RBD, REM sleep behavior disorder.

TABLE 2. *Comparison of [^{11}C]-labeled 2β-carbomethoxy-3β-(4-fluorophenyl)-tropane*

	No. samples	Age ± SD	Gender (m:f)	Caudate mean ± SD	*P*-value			Anterior Putamen mean ± SD	*P*-value			Posterior Putamen mean ± SD	*P*-value		
					SNCA dup	HYIII	AC		*SNCA* dup	HYIII	AC		*SNCA* dup	HYIII	AC
SNCA dup	4	52.8 ± 5.63	2;2	2.13 ± 0.45				1.52 ± 0.20				1.35 ± 0.11			
PD HYIII	10	66.5 ± 10.3	3;7	3.18 ± 0.31	**0.001**			2.72 ± 0.45	**0.001**			2.10 ± 0.30	**0.001**		
AC	3	53.3 ± 16.0	1;2	3.81 ± 0.27	**0.03**	**0.007**		3.98 ± 0.26	**0.03**	**0.004**		3.65 ± 0.26	**0.03**	**0.004**	
NC	7	59.4 ± 5.00	4;3	4.29 ± 0.56	**0.003**	**<0.0001**	0.09	4.44 ± 0.58	**0.003**	**<0.0001**	0.09	4.02 ± 0.40	**0.003**	**<0.0001**	0.06

Displays the comparative statistics examining differences in [^{11}C]CFT between four sample groups.
Significantly different *P*-values were highlighted in bold (significance threshold was assessed at the $P > 0.05$ level).
PD H and Y III, sporadic Parkinson's disease patients with Hoehn and Yahr stage III disease; *SNCA* dup, patients with *SNCA* duplication; AC, asymptomatic carriers; NC, normal controls.

mapping image of the ratio index was created. Statistical analysis was performed using the Mann-Whitney test.

All FDG–PET images were spatially normalized to a standard template produced by Montreal Neurological Institute using an in-house template of FDG–PET images and smoothed with Gaussian filter for 16 mm FWHM to increase the signal-to-noise ratio before statistical processing. A group effect of affected subjects (n = 4) and unaffected subjects (n = 3) was estimated in comparison with healthy control subjects using ANCOVA (analysis of covariance) statistics excluding the aging effect. We selected global normalization proportional scaling in global normalization. Statistical inference on the SPM (statistical parametric mapping) was corrected using the theory of Gaussian Fields. The threshold for SPM was set at $P < 0.05$, corrected for multiple comparisons.

Evaluation of REM Sleep Behavior Disorder

We assessed REM (rapid eye movement) sleep behavior disorder (RBD) in six affected patients (A-II-9, A-II-11, C-III-3, E-III-6, F-III-2, and G-III-1; 47.8 ± 9.21 years; m:f = 4:2) and three asymptomatic carriers (A-II-2, A-II-4, and A-III-3; 53.3 ± 16.0 years; m:f = 1:2) according to the criteria on the International Classification of Sleep Disorder (ICSD), second edition[20]; and PSG was performed using the standard package of Alice 4 (Respironics, Pittsburgh, PA). The analysis of PSG data was performed using the standard criteria of Rechtschaffen and Kales and the EEG arousals were scored using the American Sleep Disorders Academy Guidelines.[20,21] The diagnostic criteria for REM without atonia were previously described.[22]

Olfactory Testing

We studied olfactory threshold (OT), odor discrimination (OD), and odor identification (OI) in three separate subtests using standardized "Sniffin" Sticks' (Burghardt, Wedel, Germany). These protocols were previously described in detail.[23,24] Six patients (with 47.8 ± 9.22 years; m:f = 4:2) A-II-9, A-II-11, C-III-3, E-III-6, F-III-2, and G-III-1, five asymptomatic carriers (64.6 ± 16.0 years; m:f = 1:4) A-II-2, A-II-4, A-III-3, G-II-4, and G-II-5, and 22 normal controls (64.9 ± 10.1 years; m:f = 10:12). Normative values according to Hummel et al. for 51 to 80 years control: OT; male, 7.1 ± 1.7; female, 7.7 ± 2.6; OD; male, 10.6 ± 1.8; female, 10.6 ± 1.0; OI; male, 14.2 ± 1.5; female, 13.3 ± 1.5.[25] Statistical significance was set at $P < 0.05$ by